EFDA–JET–CP(08)01/04

A.C.A. Figueiredo, A. Fonseca, L. Meneses
and JET EFDA contributors

Systematic and Routine Analysis of Radial Correlation Reflectometry Data in JET

Systematic and Routine Analysis of Radial Correlation Reflectometry Data in JET

A.C.A. Figueiredo[1], A. Fonseca[1], L. Meneses[1]
and JET EFDA contributors*

JET-EFDA, Culham Science Centre, OX14 3DB, Abingdon, UK

Preprint of Paper to be submitted for publication in Proceedings of the
HTPD High Temperature Plasma Diagnostic 2008, Albuquerque, New Mexico.
(11th May 2008 - 15th May 2008)

ABSTRACT

This paper discusses a tool specially developed for the analysis of radial correlation reflectometry data in JET. The tool, which calculates the correlation length and coherent reflection from the raw data, has been designed for off-line analysis and to assist diagnostic operators. After being verified in controlled tests using theoretical signals, the tool is validated by means of a study of ITB plasmas in JET.

1. INTRODUCTION

In JET, the radial correlation reflectometry diagnostic currently produces large amounts of improved quality data after the installation of new waveguides that increased the signal to noise ratio [1], the connection to a more powerful data acquisition system with longer recording times, and the ongoing implementation of a new calibration method [2]. As instruments to analyze such data became necessary, a software tool has been developed that meets the specific diagnostic requirements and is robust and user-friendly for the systematic off-line analysis of data and to be routinely used during the experiments. In a nutshell, the tool reads and calibrates raw signals, calculates spectra and the coherence between fixed- and variable-frequency microwave channels, which are in turn used to calculate L, the radial correlation length of the microwaves [3]. The coherent reflection G, which strongly depends on the level of density fluctuations, is also calculated. Both L and G are required to determine the actual correlation length and level of turbulent plasma density fluctuations, which can be achieved by full-wave modelling of the diagnostic [4]. In the remainder of this paper, the description, verification and validation of the analysis tool are addressed in Section 2, and results are discussed in Section 3.

2. RESULTS

The radial scale of turbulence is calculated from the correlation length L of two probing microwaves from separate fixed- and variable-frequency channels. JET has four X mode reflectometer systems operating around as many different radial positions [1]. Each system measures one L from the variation of coherence with the separation between the cutoff positions of the two waves. Although the concept of spectral coherence is relatively simple [5], its practical application may not be straightforward. Indeed, coherence analysis of correlation reflectometry must be approximated and is not adequate for automatic processing, requiring considerable interaction with the calculation software. So, the tool has been implemented in IDL as simply as possible yet in a versatile way. To calculate L, the tool starts by loading and calibrating the complex signals acquired from the fixed and variable reflectometer channels.

The signals can then be filtered and coherence analysis is usually carried out on them, other possibilities being their in-phase or quadrature components, their amplitudes, or their phases. The spectral coherence $\gamma(f)$ is calculated in terms of the Fourier spectra of the complex signals from the fixed and variable frequency channels $F(f)$ and $V(f)$, respectively, assuming that density fluctuations at their cutoff

positions are stationary random processes [5], $\gamma(f) = |\langle F(f)\, V^*(f)\rangle| / \sqrt{\langle |F(f)|^2\rangle \langle |V(f)|^2\rangle}$. The average or peak of $\gamma(f)$ in a chosen frequency interval gives one value $\bar{\gamma}$ for each variable microwave probing frequency, which is stepped up or down in plateaus during the measurement. By plotting the obtained $\bar{\gamma}$ values versus the radial separation between the two cutoffs ΔR and fitting an exponential model, L is obtained as the 1/e dropping distance. The coherent reflection $G(f)$ is here calculated for the fixed channel as $G(f) = |\langle F(f)\rangle| / \sqrt{\langle |F(f)|^2\rangle}$, and likewise for the variable channel [4]. Similarly to $\gamma(f)$, a plateau value $\bar{G}$ is retrieved from $G(f)$. However, contrary to $\gamma(f)$ coherent reflection should not depend on the variable frequency plateau. Otherwise, the fluctuation level would change significantly during the measurement and the hypothesis of stationary fluctuations would fail. So, $G(f)$ should remain approximately constant during a measurement, which typically lasts about 250ms with 20ms plateaus and yields one value for L and another for G. The basic difficulty in the calculations is the realization of the ensemble averages denoted by $\langle\rangle$ in the above formulas for $\gamma(f)$ and $G(f)$. A sufficient number of instances of $F(f)$ and $V(f)$ is obtained for every plateau by time partitioning the signals with non-overlapping windows and calculating the FFT of the windowed signals. Given enough instances $G(f)$ will approach zero for a completely incoherent signal, as the sum of random phasors can then be very small. However, spectral leakage and the consequent degradation of spectral amplitude and phase do increase with the number of instances [5], and a compromise must be made. The tool allows to choose the number of instances and different window types to alleviate leakage effects. Moreover, time partitioning introduces a systematic phase increase of the signal components for consecutive time windows, which precludes the obtained spectra from forming a valid statistical ensemble. Although $\gamma(f)$ is unaffected as it involves phase *differences* between $F(f)$ and $V(f)$, the phase must be corrected for the calculation of $G(f)$. So, using the time shift property of Fourier transforms $s(t-t_0) = \mathcal{F}^{-1}[S(f) \exp(-i2\pi f\tau)]$, where $S(f) = F[s(t)]$ is the Fourier transform of s (t), for every time window $F(f)$ and $V(f)$ are multiplied by $\exp(-i2\pi f\tau)$, where τ is the difference between the window start and the respective plateau start [6]. Another consequence of leakage is that since FFT frequency bins for which there is no signal energy will not be void, there will be spurious values of $\gamma(f)$ and $G(f)$. To avoid this, $\gamma(f)$ and $G(f)$ are put to zero wherever the power spectrum falls below a predefined threshold. This zeroing also mitigates peak aliasing in $G(f)$ associated with time partitioning and phase correction, as described below. Given the significant number of choices and adjustments required by the analysis, a user-friendly graphical user interface has been created with the basic features available through controls on the main panel and menus containing many useful commands and options, for instance to ignore transients at the start of plateaus, to choose the FFT length or the number of instances of the spectra. To verify the tool and demonstrate the pitfalls in its implementation, tests are carried out with theoretical signals. As their results are known beforehand, success in these tests guarantees that the tool will work correctly with real signals, and provides indications on how to utilize it properly. Signals are sampled at 10 kHz during 1s and time partitioned to yield 21 spectra calculated with 16384 length FFTs. Except when adding noise to the variable channel, the fixed and variable

signals are the same and $G(f)$ is calculated for the variable $\gamma(f)$ and $G(f)$ should be 1, and a degradation is expected with noise addition and for nonstationary signals [7]. Figure 1(a) shows the power spectrum of a complex sinusoid with frequency 2kHz. Without zeroing it can be seen in blue in Fig. 1(b) that $\gamma(f)$ is maximum at all frequencies. The correct coherence can be seen in black after zeroing $\gamma(f)$ wherever the power spectrum falls below 10^{-3} of its maximum value. Still in Fig. 1(b), in red it is shown that adding Gaussian noise of zero mean and π standard deviation to the phase of the variable channel leads to a drastic reduction of coherence. As for $G(f)$ it was verified that, as expected, it is unaffected by stationary noise. Figure 1(c) shows in red that without phase correction coherent reflection is very low, and in blue that by correcting the phase $G(f)$ becomes practically 1. However, aliases of the true 2kHz peak appear everywhere separated by 0.021kHz, the inverse of the window duration. This effect is effectively removed by zeroing, as shown in black. In Fig.2 two signals with equally spaced components between 0.5kHz and 4.5kHz are analyzed with zeroing. With the 5 components displayed in Fig.2(a), $G(f)$ is seen in Fig.2(c) to be approximately 1 at the component frequencies and zero elsewhere. However, with 501 components as shown in Fig.2(b) $G(f)$ is much lower than expected, as seen in Fig.2(d). This is due to the small separation of the components, 8Hz, compared with the 84Hz bandwidth of the used Hann window [8], whereby leakage mixes up the phases of the components. The signal with two components at 0kHz and 2kHz shown in black in Fig.3(a) has been made nonstationary by imposing 0.2kHz sinusoidal frequency modulation [9], as seen in red. Figure 3(b) shows that $\gamma(f)$ remains 1 but occupies the spectral band of the nonstationary signal. On the contrary, it can be seen in Fig. 3(c) that $G(f)$ decreases considerably as the dense spectral composition of the nonstationary signal enhances leakage effects. As a first application and for validation purposes, the tool has been used to analyze JET plasmas with formation of an Internal Transport Barrier (ITB) [10].With $\gamma(f)$ ranging from 0.1 to 0.9, L is of the order of 1cm in the plasma core of JET plasmas without ITBs, and half that value when ITBs are formed. A clear decrease was shown of the radial correlation length in the region inside the ITB foot, which can be seen in Fig.4. This decrease is compatible with a reduction of turbulence in the plasma core, while the correlation length in the region outboard of the ITB remained unchanged, indicating that turbulence in this region is unaffected by the formation of the ITB. These conclusions agree with previous ITB studies in JET [11].

3. DISCUSSION

A tool to analyze radial correlation reflectometry data in JET has been presented and it was verified that it yields the expected results in tests performed with noiseless stationary signals, noisy, and nonstationary signals. Issues associated with spectral estimation and the realization of statistical ensembles have been adequately taken into account. Stationary noise can significantly affect $\gamma(f)$, while $G(f)$ is hindered by nonstationarity and spectral leakage. So, retrieving average or peak values from $G(f)$ must be done at spectral peaks separated by more than the characteristic leakage bandwidth. Removal of low energy spectral components in $\gamma(f)$ and $G(f)$ is essential to avoid the

appearance of spurious values. The tool has been successfully employed to study ITB plasmas in JET,10 leading to conclusions consistent with previous studies11 and thereby validating the tool.

ACKNOWLEDGMENTS

This work has been conducted under the European Fusion Development Agreement (EFDA), as well as within the framework of the Contract of Association between the European Atomic Energy Community and the Instituto Superior Técnico (IST), and it has also received financial support from the Fundação para a Ciência e a Tecnologia (FCT, Lisbon). The content of the publication is the sole responsibility of the authors and does not necessarily represent the views of the European Commission, the FCT, the IST, or their services.

REFERENCES

[1]. S. Hacquin, L. Meneses, L. Cupido, S. Sharapov, B. Alper, J. Fessey, A. Klein, D. Testa, and JET-EFDA Contributors, Rev. Sci. Instrum. **77**, 10E925 (2006).

[2]. See Poster J4 in this conference by A. Fonseca et al., *In-situ Calibration Of The Correlation Reflectometry Systems On The JET Tokamak*.

[3]. A.E. Costley, P. Cripwell, R. Prentice, and A.C.C. Sips, Rev. Sci. Instrum. **61**, 4274 (1990).

[4]. G.J. Kramer, R. Nazikian, and E. Valeo, Rev. Sci. Instrum. **74**, 1421 (2003).

[5]. J.S. Bendat and A. G. Piersol, *Engineering Applications of Correlation and Spectral Analysis* (Wiley-Interscience, New York, 1993), 2nd ed.

[6]. Notice that for stationary signals $G(f) = 1$ where $1/f$ is a submultiple of the window duration, regardless of phase correction.

[7]. Here, a signal is made nonstationary by *deterministically* time varying its spectral content and then time partitioning it. Assuming ergodicity, the spectra of the time-windowed signals are realizations of the full signal spectrum, whereby the signal becomes statistically nonstationary.

[8]. The window bandwidth is here defined as twice the frequency of the first zero of the window spectrum.

[9]. A.C.A. Figueiredo, J.P.S. Bizarro, and JET EFDA Contributors, Rev. Sci. Instrum. **77**, 10F509 (2006).

[10]. A.C.A. Figueiredo, A. Fonseca, L. Meneses, S. Hacquin, J. Fessey, E. Mazzucato, and JET EFDA contributors, in 34th EPS Conference on Plasma Phys. (Warsaw, Poland, 2007), ECA Vol.31F, P-2.149.

[11]. G.D. Conway, D.N. Borba, B. Alper, D.V. Bartlett, C. Gormezano, M.G. von Hellermann, A.C. Maas, V.V. Parail, P. Smeulders, and K.-D. Zastrow, Phys. Rev. Lett. **84**, 1463 (2000).

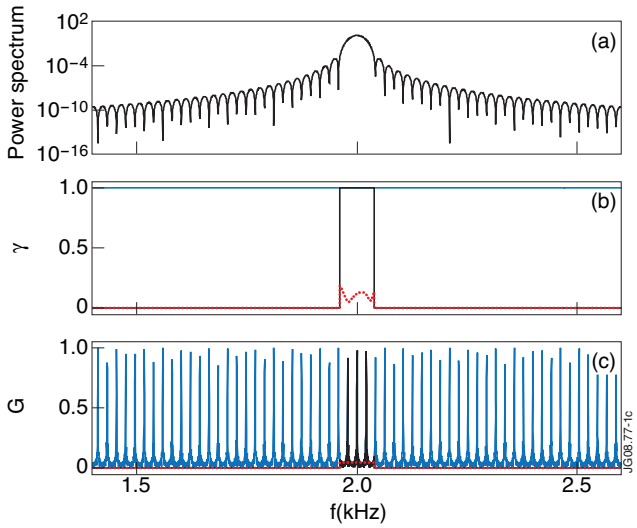

Figure 1: For the sinusoid in (a) γ(f) is shown in (b) without zeroing (blue), with zeroing (black), and with zeroing and phase noise (red). G(f) is shown in (c) without phase correction (red), with phase correction (blue), and with phase correction and zeroing (black).

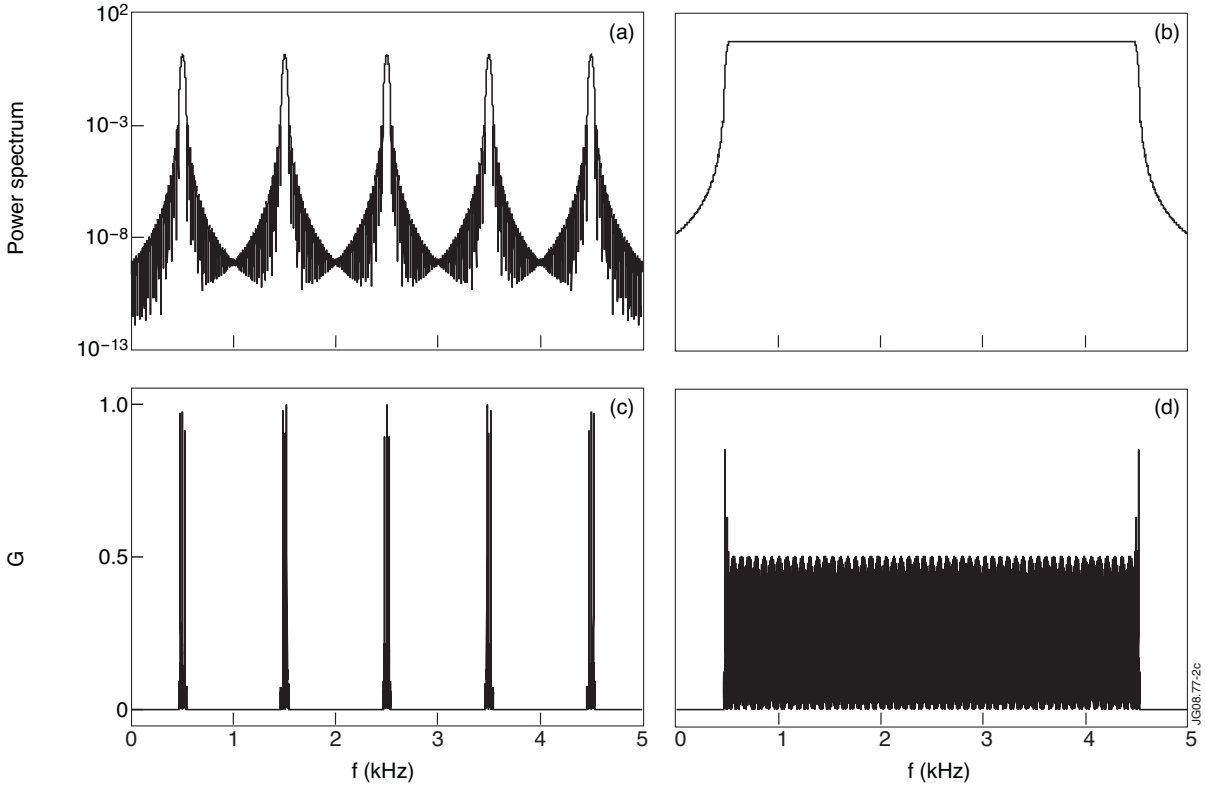

Figure 2: Analysis of two signals with (a) 5 and (b) 501 equally spaced components. With 5 components the calculated G (f) in (c) is correct, but with 501 components it is much lower than expected due to spectral leakage, as seen in (d).

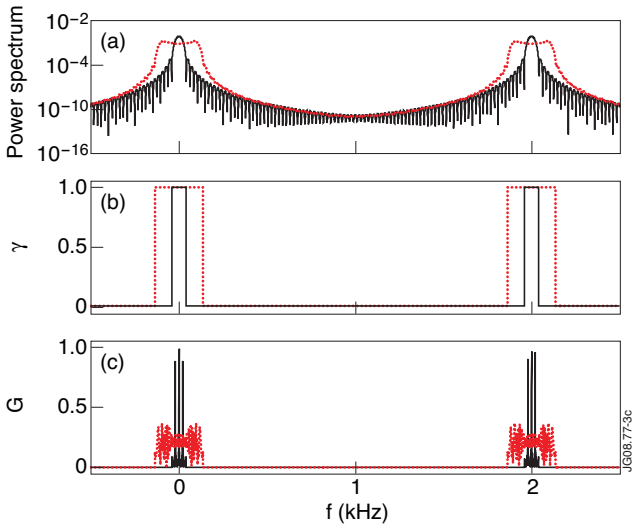

Figure 3: In (a) a signal with two components (black) is made nonstationary by imposing frequency modulation (red). While γ (f) in (b) remains 1 in the new spectral band, G(f) decreases considerably as seen in (c).

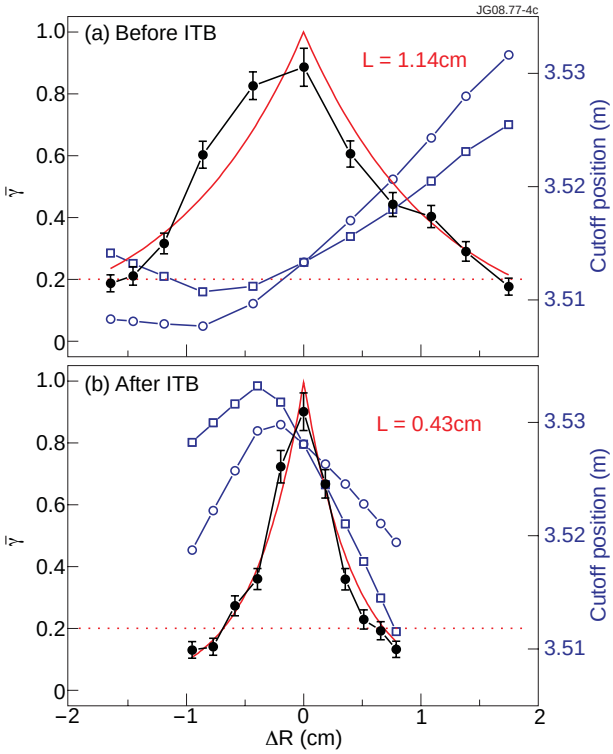

Figure 4: Application to ITB formation in JET plasmas showing the radial correlation length in the region inside the ITB foot (a) before and (b) after the ITB formation [10].